

Sinterability of $\text{ZrSiO}_4/\alpha\text{-Al}_2\text{O}_3$ mixed powders

Shi-Ke Zhao^{a,*}, Yong Huang^a, Chang-An Wang^a, Xiao-Xian Huang^b, Jing-Kun Guo^b

^aThe State Key Lab of New Ceramics and Fine Processing, Department of Materials Science and Engineering, Tsinghua University, Beijing 100084, China

^bThe State Key Lab on High Performance Ceramics and Superfine Microstructure, Shanghai Institute of Ceramics, Chinese Academy of Sciences, Shanghai 200050, China

Received 27 March 2002; received in revised form 6 May 2002; accepted 3 June 2002

Abstract

The sinterability of $\text{ZrSiO}_4/\alpha\text{-Al}_2\text{O}_3$ mixed powders with three different compositions was investigated with respect to phase development during firing. The study reveals that the 65/35 sample (low- Al_2O_3) has good sinterability below the temperature of 1450 °C because it contains more easily sintered $\text{ZrSiO}_4/\alpha\text{-Al}_2\text{O}_3$ particle interfaces. With increasing temperature and the reaction proceeding, $\text{ZrSiO}_4/\alpha\text{-Al}_2\text{O}_3$ particle interfaces disappeared and the sinterability of samples was changed greatly by the phase developments. As a result, the 80/20 sample (high- Al_2O_3) became more sinterable at high temperatures. SEM observations show a smaller ZrO_2 grain size in the 80/20 sample than in the 65/35 sample, because ZrO_2 grain growth in the 80/20 sample involved longer diffusion paths.

© 2002 Elsevier Science Ltd and Techna S.r.l. All rights reserved.

Keywords: A. Sintering; C. Diffusion; D. Mullite; $\text{ZrSiO}_4/\alpha\text{-Al}_2\text{O}_3$ mixed powders

1. Introduction

Mullite is considered a promising candidate for high-temperature structural applications because of its relatively low thermal expansion coefficient, good creep resistance, excellent high-temperature strength and chemical stability [1–3]. Mullite, however, has low fracture toughness and relatively low strength at room temperature, when compared with other engineering ceramics. Mullite-based composites with dispersed zirconia particles have been widely studied to overcome these disadvantages.

Reaction sintering of $\text{ZrSiO}_4/\alpha\text{-Al}_2\text{O}_3$ mixed powders is an easy and inexpensive route to obtain homogeneous mullite–zirconia composites with enhanced mechanical properties [4–8]. However, the fully dense compacts are difficult to achieve, due to the poor sinterability of the mixed powders. In reaction sintering of $\text{Al}_2\text{O}_3/\text{SiO}_2$ mixtures, it has been shown that the sinterability is strongly dependent on the $\text{Al}_2\text{O}_3/\text{SiO}_2$ ratio, and good sinterability requires a low $\text{Al}_2\text{O}_3/\text{SiO}_2$ ratio [9,10]. Similarly, $\text{ZrSiO}_4/\alpha\text{-Al}_2\text{O}_3$ ratio should also have a great

influence on the sinterability of $\text{ZrSiO}_4/\alpha\text{-Al}_2\text{O}_3$ mixed powders because the sinterability of the two powders is different. However, the influence has not been particularly documented so far, although other factors affecting the sinterability have been reported by many workers [5–7].

In the present work, we prepared mullite–zirconia multiphase ceramics from reaction sintering of $\text{ZrSiO}_4/\alpha\text{-Al}_2\text{O}_3$ with three different $\text{ZrSiO}_4/\alpha\text{-Al}_2\text{O}_3$ ratios and examined the sinterability of the mixed powders by investigating the densification process and phase development during firing.

2. Experimental procedures

All the samples were prepared starting from high-purity (99.9%) alumina and fine zircon powders (99%). Average particle sizes were 0.35 and 0.48 μm , respectively. The main impurities of the zircon were Al_2O_3 (0.50 wt.%), CaO (0.40 wt.%) and Fe_2O_3 (<0.10 wt.%). The sample compositions are expressed by the weight ratios of Al_2O_3 to SiO_2 in ZrSiO_4 . Using polyvinyl alcohol (PVA) as a binder, the powders with $\text{Al}_2\text{O}_3/\text{SiO}_2$ weight ratios of 65/35, 71.8/28.2, and 80/20

* Corresponding author. Tel.: +86-10-6278-5488; fax: +86-10-6277-2857.

E-mail address: zhaoskire@tsinghua.edu.cn (S.-K. Zhao).

were then ball-milled in distilled water for 24 h to obtain homogeneous mixtures. After drying at 120 °C and screening (120 mesh), the obtained mixtures were dry-pressed and then isostatically pressed at 200 MPa to form green compacts, which were subsequently sintered in air at different temperatures.

The bulk density and open porosity of sintered compacts were measured by the Archimedes' method. Phase development during firing was characterized by XRD, with Ni filtered $\text{CuK}\alpha$ radiation (D/max-ra diffractometer, Japan). Microstructures of polished sintered compacts were observed with scanning electron microscopy (SEM; EPMA-870QH, Shimadzu, Japan). Thermal etching was performed on the sintered compacts at a temperature 100 °C below sintering temperature for 1 h before SEM observations.

3. Results and discussion

3.1. Densification process

Fig. 1 shows the linear shrinkage curves of three samples with different compositions during firing (which are respectively designated as 65/35, 71.8/28.2 and 80/20 sample according to their $\text{Al}_2\text{O}_3/\text{SiO}_2$ weight ratios in the following). As can be observed, there are some differences between the three curves although they are roughly similar. The open porosities of these three samples with increasing temperature are also different as shown in Fig. 2. These results are indicative of their different sinterability.

We can consider that there exist three types of interfaces with different sinterability in all the compacts before mullite begins to form, they are the particle interfaces of $\text{ZrSiO}_4/\text{ZrSiO}_4$, $\text{ZrSiO}_4/\alpha\text{-Al}_2\text{O}_3$, and $\alpha\text{-Al}_2\text{O}_3/\alpha\text{-Al}_2\text{O}_3$, respectively. It has been shown, at a certain

sintering temperature, solid state reaction between ZrSiO_4 and $\alpha\text{-Al}_2\text{O}_3$ would take place and form amorphous aluminosilicate phase at $\text{ZrSiO}_4/\alpha\text{-Al}_2\text{O}_3$ particle interfaces, and this amorphous phase could promote densification markedly via viscous flow [11]. In addition, as it is generally known, $\alpha\text{-Al}_2\text{O}_3$ powder is more sinterable than ZrSiO_4 powder. So it could be tentatively supposed, of these three various interfaces, $\text{ZrSiO}_4/\alpha\text{-Al}_2\text{O}_3$ particle interface possesses the best sinterability; $\alpha\text{-Al}_2\text{O}_3/\alpha\text{-Al}_2\text{O}_3$ interface takes second place, and $\text{ZrSiO}_4/\text{ZrSiO}_4$ interface the poorest. The sinterability of the compacts is mainly dependent on the ratios of these three types of particle interfaces, and more desirable sinterability should be anticipated if the compacts contain more $\text{ZrSiO}_4/\alpha\text{-Al}_2\text{O}_3$ particle interfaces.

According to their average particle sizes and theoretical densities, the specific surfaces of ZrSiO_4 and $\alpha\text{-Al}_2\text{O}_3$ powders can be estimated to be about 1.34 and 2.16 m^2/g , respectively (here a spherical particle shape has been assumed). In the compacts of 100 g with different compositions, the total surface areas of ZrSiO_4 and $\alpha\text{-Al}_2\text{O}_3$ particles are calculated and given in Table 1. As can be seen, the total surface area of ZrSiO_4 particles in the 65/35 samples is nearly equal to that of $\alpha\text{-Al}_2\text{O}_3$ particles, which means that more $\text{ZrSiO}_4/\alpha\text{-Al}_2\text{O}_3$ particle interfaces should be formed. A good sinterability should be achieved for this sample, if the powders are completely homogeneously mixed. In contrast, the difference of total surface area of ZrSiO_4 and $\alpha\text{-Al}_2\text{O}_3$ particles is the largest in the 80/20 sample, which is thus supposed to have the poorest sinterability. For the same reason, the 71.8/28.2 sample has an intermediate sinterability. These considerations can explain reasonably the porosity changes of the samples with different $\text{Al}_2\text{O}_3/\text{SiO}_2$ ratios below 1450 °C.

As shown in Fig. 2, in the temperature range lower than 1450 °C, the 65/35 sample shows the lowest porosity, and the 80/20 samples have the highest porosity. These results are also consistent with the linear shrinkage curves shown in Fig. 1. However, it becomes different at higher temperatures. The porosity of 80/20 sample decreased more rapidly than those of 65/35 and 71.8/28.2 samples and turned into the lowest one when the temperature reached 1600 °C. Furthermore, the 65/35 and 71.8/28.2 samples exhibited a volume expansion when the temperature exceeded 1450 °C, which can be seen from the shrinkage changes in Fig. 1. As it will be

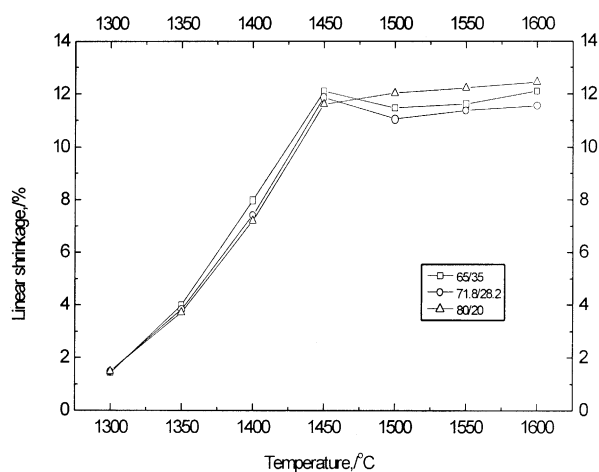


Fig. 1. Linear shrinkage curves of the samples with different $\text{Al}_2\text{O}_3/\text{SiO}_2$ ratios.

Table 1

Total surface areas (m^2) of ZrSiO_4 and $\alpha\text{-Al}_2\text{O}_3$ particles in the compacts (100 g) with different compositions

$\text{Al}_2\text{O}_3/\text{SiO}_2$	65/35	71.8/28.2	80/20
ZrSiO_4	83.0	72.8	57.8
$\alpha\text{-Al}_2\text{O}_3$	81.7	98.2	122.5

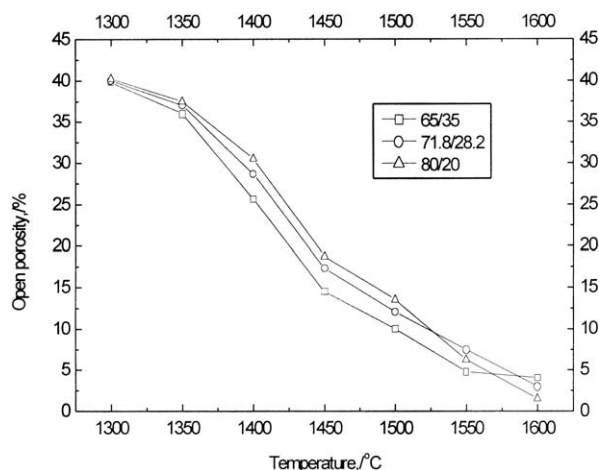


Fig. 2. Open porosity changes of the samples with different $\text{Al}_2\text{O}_3/\text{SiO}_2$ ratios during firing.

shown in the following, these can be interpreted in terms of their phase developments with increasing temperature.

3.2. Phase development

Figs. 3 and 4 show the phase developments of three various samples during firing. ZrO_2 peaks are observed in the 80/20 sample at 1350 °C, while at the same temperature no ZrO_2 peaks appear in the 65/35 sample. As it is well-known, pure zircon usually dissociates at a temperature higher than 1600 °C. But in the present study, zircon dissociation was initiated by Al_2O_3 , and could take place at a low temperature to 1350 °C. In the 80/20 sample containing more Al_2O_3 , the dissociation

process would be effectively enhanced, and thus more ZrO_2 could be formed. Although ZrO_2 could be also formed in the 65/35 sample, it is undetectable by XRD because its amount is very small.

With the temperature increasing to 1450 °C, mullite peaks are observed in the 80/20 sample, while, for the 65/35 sample, mullite first appeared at 1500 °C, suggesting the $\text{Al}_2\text{O}_3/\text{SiO}_2$ ratios have an influence on the temperature for the onset of mullization. This is consistent with the study on mullization of $\alpha\text{-Al}_2\text{O}_3/\text{silica}$ microcomposite powders by Sacks et al. [12], where they found that initial mullization in an Al_2O_3 -rich sample began at lower temperature. In their study, the mullite formation during the first stage was controlled by the dissolution of Al_2O_3 in the siliceous phase, and a smaller amount of Al_2O_3 needs to be dissolved in the SiO_2 to attain the critical nucleation concentration (CNC) for mullite in Al_2O_3 -rich sample. As a result, a lower temperature is needed to initialize the mullization. In the previous work [11], it has been tentatively shown that mullite grains mainly nucleate and grow from non-crystalline matrix in the reaction sintering of $\text{ZrSiO}_4/\alpha\text{-Al}_2\text{O}_3$. The initial mullization may be also controlled by a similar mechanism to that supposed by Sacks et al. [12].

The reaction was almost completed in the 65/35 and 80/20 samples when the temperature reached 1550 °C, which is indicated by the very low intensities of $\alpha\text{-Al}_2\text{O}_3$ peaks in Fig. 3 and ZrSiO_4 peaks in Fig. 4. The 65/35 sample mainly consists of mullite, ZrO_2 and ZrSiO_4 phases, and the 80/20 sample mainly mullite, ZrO_2 and $\alpha\text{-Al}_2\text{O}_3$ phases. According to the earlier discussion, the 80/20 sample is expected to become more sinterable

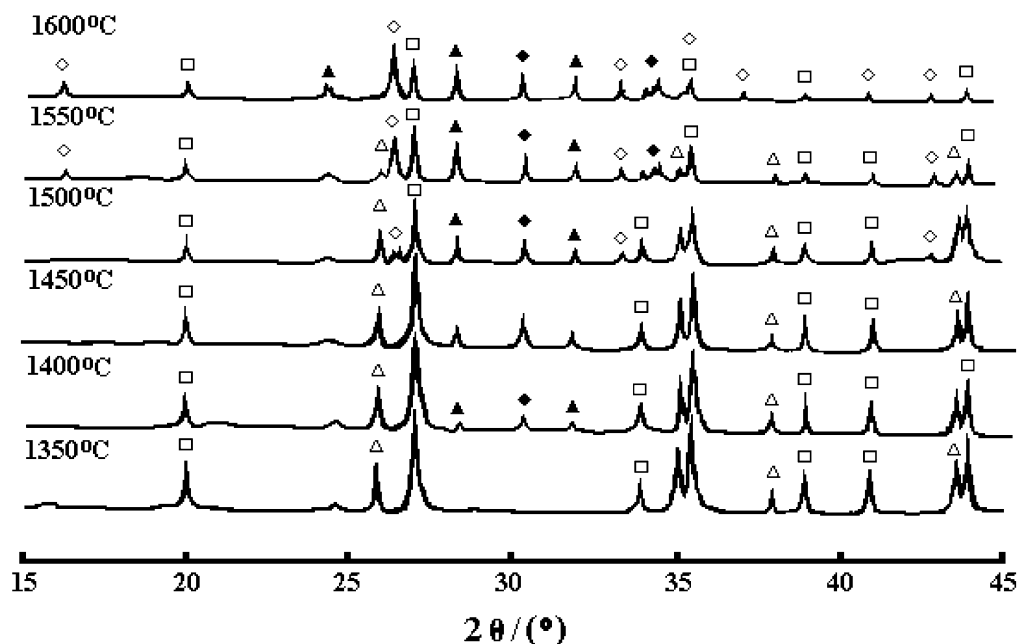


Fig. 3. Phase development of the 65/35 samples during sintering (\square : ZrSiO_4 ; \triangle : $\alpha\text{-Al}_2\text{O}_3$; \blacklozenge : t- ZrO_2 ; \blacktriangle : m- ZrO_2 ; \diamond : mullite).

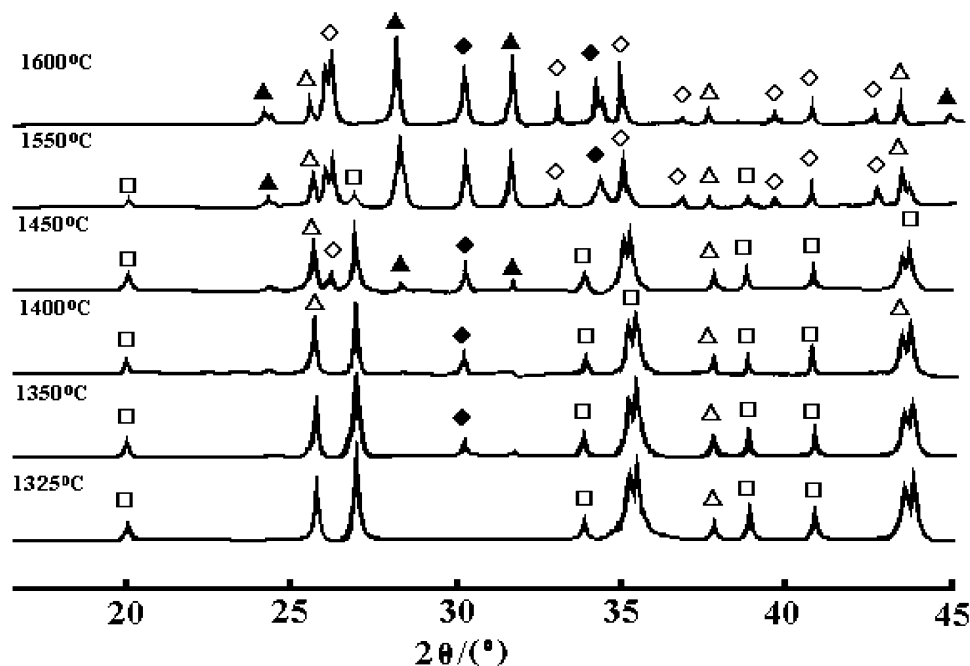


Fig. 4. Phase development of the 80/20 samples during sintering (□: ZrSiO_4 ; △: $\alpha\text{-Al}_2\text{O}_3$; ◆: t-ZrO_2 ; ▲: m-ZrO_2 ; ◇: mullite).

than 65/35 sample above 1550 °C, which can be used to explain the lower porosity of the 80/20 sample. The porosity changes are also consistent with the shrinkage differences between the three samples in this temperature range (shown in Fig. 1). In addition, the volume expansion associated with mullite formation is also responsible for the shrinkage differences earlier. The volume expansion values of these three samples are about 11.8% (65/35 sample), 14% (71.8/28.2 sample) and 10.9% (80/20 sample) respectively, when a complete mullization is achieved. Fig. 1 shows that the high

shrinkage of the 80/20 sample is in good agreement with its low volume expansion.

3.3. Microstructure observations

Fig. 5 shows the microstructures of the 65/35 and 80/20 samples sintered at 1600 °C for 2 h. As it can be seen, the ZrO_2 grain (white grains) in the 80/20 sample is obviously smaller than that in the 65/35 sample. This indicates that the compositions had a significant effect on the ZrO_2 grain growth during firing. In the 80/20

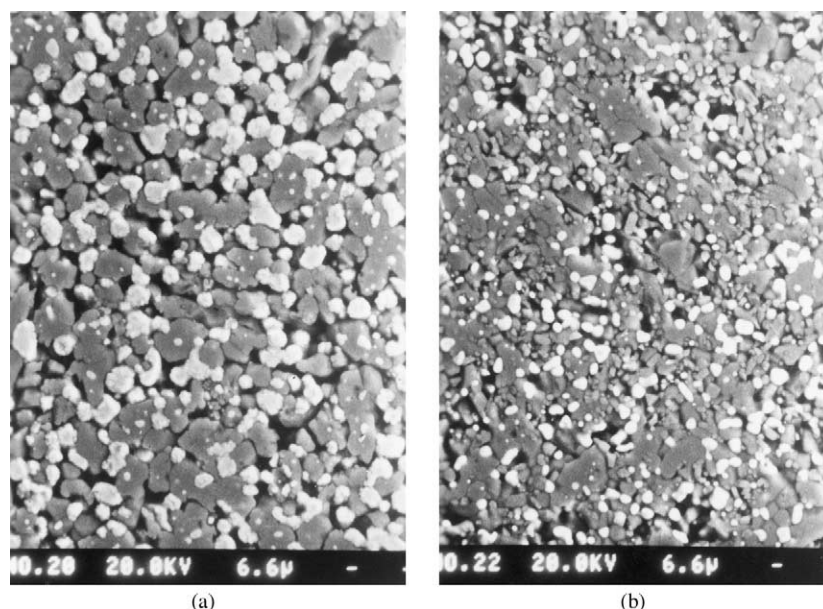


Fig. 5. SEM micrographs from the polished surface (thermally etched) of the samples (a) 65/35; (b) 80/20.

sample containing more α -Al₂O₃, the ZrO₂ from ZrSiO₄ dissociation would be more completely surrounded and isolated by the amorphous aluminosilicate phase, which was formed from the solid reaction between ZrSiO₄ and α -Al₂O₃. The amorphous phase could also effectively inhibit ZrO₂ grain growth. In addition, ZrO₂ concentration of the 80/20 sample is smaller compared with the 65/35 sample, and ZrO₂ grain growth needs to involve longer diffusion paths, thus leading to a smaller grain size.

4. Conclusion

The sinterability of ZrSiO₄/ α -Al₂O₃ mixed powders is closely related to the compositions and also the reaction progress. At temperatures lower than 1450 °C, below which mullitization has not taken place, the sinterability is mainly dependent on the ratios of three various particle interfaces (i.e. ZrSiO₄/ZrSiO₄, ZrSiO₄/ α -Al₂O₃, and α -Al₂O₃/ α -Al₂O₃ particle interfaces). The 65/35 sample (low-Al₂O₃) shows good sinterability below the temperature of 1450 °C, which can be attributed to more sinterable ZrSiO₄/ α -Al₂O₃ particle interfaces than in the 80/20 sample. However, the sinterability of samples changed with the reaction proceeding, and it is primarily controlled by the respective sinterability of ZrSiO₄ and α -Al₂O₃ powders. The 80/20 sample (high-Al₂O₃) became easier to sinter than the 65/35 sample (low-Al₂O₃) when mullitization was almost completed, because α -Al₂O₃ powder has better sinterability than ZrSiO₄ powder. ZrO₂ grain size in the 80/20 sample is smaller than in the 65/35 sample, for ZrO₂ grain growth in the 80/20 sample need to involve a relatively longer diffusion paths.

References

- [1] D.X. Li, W.J. Thompson, Kinetics mechanisms for mullite formation from sol–gel precursors, *J. Am. Ceram. Soc.* 73 (1990) 1963–1968.
- [2] G.M. Anikumar, U.S. Hareesh, A.D. Damodaran, K.G.K. Warriar, Effect of seeds on the formation of sol–gel mullite, *Ceram. Int.* 23 (1997) 537–543.
- [3] P.C. Dokko, J.A. Pask, K.S. Mazdiasni, High temperature mechanical properties of mullite under compression, *J. Am. Ceram. Soc.* 60 (1977) 150–155.
- [4] P. Descamps, S. Sakaguchi, M. Poorteman, F. Cambier, High-temperature characterization of reaction-sintered mullite–zirconia composites, *J. Am. Ceram. Soc.* 74 (1991) 2476–2481.
- [5] F. Cambier, C. Baudin delalastra, P. Pilate, A. Leriche, Formation of microstructural defects in mullite–zirconia and mullite–alumina–zirconia composites obtained by reaction-sintering of mixed powders, *Br. Ceram. Trans.* 83 (1984) 196–200.
- [6] T. Koyama, S. Hayashi, A. Yasumori, K. Okada, M. Schmucker, H. Schneider, Microstructure and mechanical properties of mullite/zirconia composites prepared from alumina and zircon under various firing conditions, *J. Eur. Ceram. Soc.* 16 (1996) 231–237.
- [7] N. Claussen, J. Jahn, Mechanical properties of sintered, in situ-reacted mullite–zirconia composites, *J. Am. Ceram. Soc.* 63 (1980) 228–229.
- [8] J.M. Wu, C.M. Lin, Effect of CeO₂ on reaction-sintered mullite–ZrO₂ ceramics, *J. Mater. Sci.* 26 (1991) 201–206.
- [9] M.D. Sacks, J.A. Pask, Sintering of mullite-containing materials I: effect of composition, *J. Am. Ceram. Soc.* 65 (1982) 65–70.
- [10] M.D. Sacks, J.A. Pask, Sintering of mullite-containing materials II: effect of agglomeration, *J. Am. Ceram. Soc.* 65 (1982) 70–77.
- [11] S.K. Zhao, X.X. Huang, J.K. Guo, The effect of mullite seeding on reaction-sintered mullite–zirconia multiphase ceramic, *J. Mater. Sci. Lett.* 19 (2000) 707–710.
- [12] M.D. Sacks, K. Wang, G.W. Scheiffele, N. Bozkurt, Effect of composition on mullite behavior of α -alumina/silica micro-composite powders, *J. Am. Ceram. Soc.* 80 (1997) 663–672.